Towards clinical implementation of quantitative PET and SPECT imaging

Burgt, A. van de

CHAPTER 3

Investigating the potential added value of [^{18}F]FDG-PET/CT in long COVID patients with persistent symptoms: a proof of concept study

Authors

L. L. Chen, A. van de Burgt**, F. Smit , R.S. Audhoe,
S.M. de Boer, F.H.P. van Velden and L.F. de Geus-Oei

** L. L. Chen and A. van de Burgt contributed equally to this work and share first authorship.*

Published

Nuclear Medicine Communications, 2023; 44(6): 495-501,
DOI: 10.1097/MNM.0000000000001689

Supplementary materials

https://doi.org/10.1097/MNM.0000000000001689

ABSTRACT

Objective

Since the end of 2019, the SARS-CoV-2 virus has infected millions of people, of whom a significant group suffers from sequelae from coronavirus disease (COVID-19), termed long COVID. As more and more patients emerge with long COVID who have symptoms of fatigue, myalgia and joint pain, we must examine potential biomarkers to find quantifiable parameters to define the underlying mechanisms and enable response monitoring. The aim of this study is to investigate the potential added value of [18F]FDG-PET/CT for this group of long COVID patients.

Methods

For this proof of concept study, we evaluated [18F]FDG-PET/CT scans of long COVID patients and controls. Two analyses were performed: semi-quantitative analysis using target-to-background ratios (TBR) in 24 targets and total vascular score (TVS) assessed by two independent nuclear medicine physicians. Mann-Whitney U-test was performed to find significant differences between the two groups.

Results

13 patients were included in the long COVID group and 25 patients were included in the control group. No significant differences ($p < 0.05$) were found between the long COVID group and the control group in the TBR or TVS assessment.

Conclusion

As we found no quantitative difference in the TBR or TVS between long COVID patients and controls, we are unable to prove that [18F]FDG is of added value for long COVID patients with symptoms of myalgia or joint pain. Prospective cohort studies are necessary to understand the underlying mechanisms of long COVID.

Keywords

inflammation, infection, vasculitis, SARS-CoV-2, imaging

INTRODUCTION

Since the end of 2019, the severe acute respiratory syndrome coronavirus 2 (SARS-CoV-2) virus has been disrupting lives globally despite extensive efforts to contain the virus [1]. The most common symptoms of acute coronavirus disease 2019 (COVID-19) are fever, dry cough and fatigue, albeit the disease expression is highly heterogeneous [1–4]. About 80% of the patients experience mild to moderate disease, whilst 5% develop critical illness [5,6]. Moreover, the majority of patients develop sequelae after recovering from the acute SARS-CoV-2 infection that lasts for weeks to months [7]. This is called long COVID, or post-COVID syndrome [6,8,9]. Symptoms associated with long COVID include fatigue, dyspnea, poor memory, hair loss, joint pain, attention disorder and myalgia, although this disease expression is also heterogeneous [4,10]. The onset of arthritis and vasculitis has also been reported in long COVID patients, and there is a growing recognition that COVID-19 is a vascular disease that leads to an escalating cascade of inflammatory pathways [11–14].

Long COVID patients are often PCR-negative and show no radiological or biochemical abnormalities. The lag of clinical recovery can be exasperating, which causes mental problems on top of the physical problems [6]. As the primary focus of the pandemic was to investigate the optimal treatment for acute COVID-19 patients and deal with the latest mutations of SARS-CoV-2, optimizing the rehabilitation of long COVID patients lagged. As a result, clear guidelines on the optimal treatment for long COVID patients are lacking [4].

As more and more patients with COVID in the medical history are emerging with vague symptoms, e.g. fatigue, joint pain and myalgia similar to vasculitis, sarcoidosis and polymyalgia rheumatica (PMR), there is a need for (imaging) biomarkers to find quantifiable parameters in order to define the underlying mechanisms. As a result, this would enable evaluation of disease activity and treatment response monitoring. 18-F-2-fluoro-2-deoxyglucose ([^{18}F]FDG) positron emission tomography/computed tomography (PET/CT) can potentially be of added value in this process, as [^{18}F]FDG-PET/CT is able to determine localized metabolic activity, including infection, inflammation and malignancies [15]. Abnormal [^{18}F]FDG-PET/CT scans in long COVID patients have been observed in earlier studies, albeit no study has been able to discern a typical visual [^{18}F]FDG-uptake pattern in long COVID patients yet, which shows the need for further investigation [16–18]. This study aims to investigate the potential added value of [^{18}F]FDG-PET/CT for long COVID patients with persistent symptoms such as myalgia, joint pain and fatigue, reminiscent of vasculitis, sarcoidosis and PMR.

METHODS

Study design and population

To investigate the potential added value of [18F]FDG-PET/CT for long COVID patients with persistent symptoms, we performed a retrospective proof of concept study to qualitatively and quantitatively compare [18F]FDG-PET/CT scans of long COVID patients and controls.

For the long COVID patient group, we included patients from our long COVID outpatient clinic who presented with symptoms of myalgia or joint pain, reminiscent of vasculitis, PMR or sarcoidosis, for whom an [18F]FDG-PET/CT scan was performed between May 2021 and October 2021. This study was retrospective and approval by the medical ethics committee was therefore not required according to the Dutch law. Nevertheless, written informed consent was obtained from all participants.

For the control group, we included patients who either i) had a malignancy in the past for which they were exclusively surgically curatively treated and for whom a routine [18F]FDG-PET/CT follow-up scan was performed, excluding recurrent/residual disease; or ii) received an [18F]FDG-PET/CT scan for a suspected malignancy or etiology of unknown origin, which did not show any disease. Moreover, we exclusively included [18F]FDG-PET/CT scans from June 2019 until October 2021, as the hospital acquired a new PET/CT scanner in June 2019. We did not include patients in the control group who had received systemic oncological treatment or radiotherapy in the past or had inflammatory diseases such as sarcoidosis, vasculitis, rheumatic diseases or COVID-19 in their medical history.

Baseline information was gathered from the electronic health records consisting of sex, age, BMI, pre-PET glycaemia, administered [18F]FDG activity, interval time between [18F]FDG administration and scan acquisition, and medicine use. Differences in age, BMI, pre-PET glycaemia, administered [18F]FDG activity and interval time between [18F]FDG administration and scan acquisition were investigated with an unpaired two-tailed Student's t-test and differences in sex using a Chi-squared test. We considered $p < 0.05$ to be significant.

Data collection

We anonymized patient data and recorded these in a database. Whole-body [18F]FDG-PET/CT was performed for long COVID patients on the 5-Ring Discovery MI PET/CT (GE Healthcare, Chicago, IL, USA) [19]. Control [18F]FDG-PET/CT scans were acquired as whole-body images if available and as torso (mid-thigh to skull base) images if no whole-body images were available. Data acquisition was performed approximately 60 min after intravenous [18F]FDG administration (1.5 MBq per kilogram bodyweight if BMI < 30, 2.1 MBq per kilogram bodyweight if BMI > 30). Of note, due to use of a highly sensitive

PET/CT system this dose is lower than the standard 3.0 MBq per kilogram bodyweight. An emission scan was obtained using multiple bed positions (50% overlap between bed positions, 75 sec per bed position) [19]. Time-of-flight PET data were reconstructed using the point spread function and CT-based attenuation correction (120 kV, smart mA modulations with a noise index of 49.5 and an mA ranging from 15 to 550, 0.5 sec rotation time). Body-weighted standardized uptake values (SUV) were obtained using Sectra IDS7 (Sectra AB, Linköping, Sweden) (PACS).

Data analysis

To compare long COVID patients with controls, a semi-quantitative analysis was performed by determining the target-to-background ratio (TBR) according to the nine research targets described in the European Association for Nuclear Medicine (EANM) recommendations for [^{18}F]FDG-PET/CT imaging in large vessel vasculitis (LVV) and PMR to account for the variability of SUV values: the carotid, subclavian, axillary, vertebral, and pulmonary arteries, the ascending, descending, and abdominal aorta, and the aortic arch [20–23]. Additional targets consisted of the parotid glands, external iliac arteries, femoral arteries, tibial arteries, the liver and the brachioradialis muscle. The background was calculated as the average SUV in the vena cava inferior and vena cava superior (figure 1).

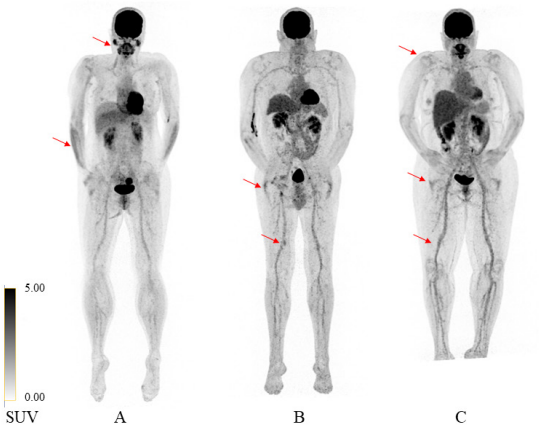

Figure 1. Examples of three long COVID patients with persistent symptoms of fatigue, myalgia or joint pain. (A) High to moderate [^{18}F]FDG-uptake in the m. brachioradialis and parotid glands (red arrows). (B and C) Low to moderate [^{18}F]FDG-uptake in joints and vessels in the lower extremities (red arrows).

In order to assess the difference in overall [^{18}F]FDG-uptake between the long COVID group and control group, we used the total vascular score (TVS), as this takes heterogeneity within groups into account. The TVS was determined using the seven clinical targets

described in the EANM recommendations for [18F]FDG-PET/CT imaging in LVV and PMR: thoracic aorta, abdominal aorta, subclavian arteries, axillary arteries, carotid arteries, iliac arteries and femoral arteries [22]. Additional targets consisted of the parotid glands, shoulder girdle, and hip girdle (analysis of 10 targets, performed on all patients). Additionally, the tibial arteries, lower arm muscles and hands were assessed if visible on the scan (analysis of 13 targets, performed on patients with total body scans). A standardized 0-to-3 grading system was used to assess all targets, and was defined as follows: 0 = physiological [18F]FDG-uptake; 1 = minimally heightened [18F]FDG-uptake (< mediastinum), 2 = clearly increased [18F]FDG-uptake (≥ mediastinum and < liver), 3 = very marked [18F]FDG-uptake (≥ liver). The ten or thirteen targets per patient were assessed independently by two experienced nuclear medicine physicians (SB, RA) who were blinded. The TVS was calculated as the sum of all target scores.

Statistical analysis

For the semi-quantitative analysis, the mean, median, standard deviation and range were calculated for every TBR and subject (Supplementary table A). We performed the Mann-Whitney U-test to assess the difference between the long COVID group and control group for each target and applied Bonferroni correction for multiple testing [24]. We considered a p-value < 0.05 to be statistically significant.

For the TVS analysis, the interclass correlation (ICC) was determined to assess intra-observer similarity. A threshold of ICC < 0.75 was agreed upon to analyze the two observers separately. A separate Mann-Whitney U test was performed for all subjects using ten targets (maximum number of subjects) and subjects with thirteen targets (maximum number of targets). We considered a p-value < 0.05 to be statistically significant. We used Excel (Version 2109; Microsoft, Albuquerque, NM, USA) for data collection and Matlab (version R2019b; MathWorks, Natick, MA, USA) to perform the statistical tests.

RESULTS

Patient characteristics

13 patients were included in the long COVID group and 25 patients were included in the control group (follow-up after melanoma *n* = 10, disproved suspicion of malignancy *n* = 8, follow-up after mammary carcinoma *n* = 2, follow-up after colon carcinoma *n* = 2, other indications *n* = 3). The long COVID group was on average significantly younger than the control group (47.2 ± 13.09 versus 58 ± 15.62, respectively, p = 0.017) and consisted of less males (38.5% versus 46.2%, respectively, p = 0.010). Table 1 summarizes the baseline characteristics of both groups.

[^{18}F]FDG PET/CT parameters

We found no significant differences between the long COVID and control group with regards to pre-PET glycaemia (5.33 ± 1.31 versus 5.96 ± 1.91 mmol/L, p = 0.23), administered [^{18}F]FDG activity (123.87 ± 34.35 versus 132.93 ± 38.46 MBq, p = 0.58) and interval time between [^{18}F]FDG injection and image acquisition (51.38 ± 8.49 [range 41-74] versus 48.52 ± 5.96 [range 40-68] minutes, p = 0.44) (Table 1).

Clinical data

Long COVID patients in this study reported symptoms of fatigue, dyspnea, concentration problems, myalgia, asthenia, and low mood. The severity of the COVID-19 infection ranged from mild to severe. Symptoms during infection included fatigue, dyspnea, cough, fever, myalgia, and loss of taste or smell. The time interval between COVID-19 infection and [^{18}F]FDG-PET/CT scan was 9.0 ± 4.4 months. None of the 13 long COVID patients were admitted to the hospital for the COVID-19 infection.

TBR [^{18}F]FDG-PET/CT analysis

Table 2 shows the results of the semi-quantitative analysis of all targets. No targets differed significantly between the long COVID group compared to the control group. Increased [^{18}F]FDG-uptake of the parotid glands was observed in 6/13 long COVID patients and 6/26 control patients ($TBR_{parotid}$ gland left = 1.34 versus 1.02, respectively, p = 5.52 and $TBR_{parotid}$ gland right = 1.37 versus 1.01, respectively, p = 3.35). We also observed a higher [^{18}F]FDG-uptake in the liver in the long COVID group than in the control group (TBR_{liver} = 1.47 versus 1.34, respectively, p = 0.18).

Table 1. Baseline subject characteristics.

	Long COVID (n=13)	Controls (n=25)	p-value
Gender (male, %)	5 (38.5%)	11 (44%)	0.016
Age (mean, std, yr)	47.2 (13.09)	57.3 (15.5)	0.024
BMI status (mean, std, kg/m^2)	24.11 (4.09)	24.62 (3.89)	0.89
Pre-PET glycaemia (mmol/L)	5.33 (1.31)	5.96 (1.91)	0.23
Administered [^{18}F]FDG activity (MBq)	123.87 (34.35)	132.93 (38.46)	0.58
interval time between [^{18}F]FDG injection and image acquisition (min)	51.38 (8.49)	48.52 (5.96)	0.44
Symptoms			
Fatigue	13	0	
Pain	6	0	
Dyspnoea	4	0	
Loss of strength	3	0	

Table 1. Baseline subject characteristics. (continued)

	Long COVID (n=13)	Controls (n=25)	p-value
Comorbidities (n)			
No	2	4	
Diabetes	1	5	
Hypertension	2	2	
Chronic respiratory disease	3	4	
Concomitant medications (n)			
None	5	9	
Beta-blockers	0	4	
Calcium antagonists	0	3	
Sartans	0	1	
ACE inhibitors	1	2	
Diuretics	0	1	
Oral anticoagulants	1	2	
Antiplatelet drugs	0	1	
Hypoglycaemic drugs	1	3	
Corticosteroids	2	3	
Statins	1	4	
NSAIDs	3	3	
Benzodiazepines	1	2	
Proton pump inhibitors	4	5	
Bronchodilators	2	2	

BMI = body mass index; ACE = angiotensin-converting enzyme; NSAIDs = non-steroidal anti-inflammatory drugs.

Table 2. Results of semi-quantitative analysis in the long COVID group and control group.

	TBR mean (std)		
	Long COVID (n=13)	**Controls (n=25)**	**p-value**
a. carotis communis sinistra (mean, std)	1.06 (0.16)	0.99 (0.25)	**4.97**
a. carotis communis dextra	1.04 (0.18)	1.03 (0.18)	**21.07**
a. subclavia sinistra	0.91 (0.16)	0.94 (0.15)	**11.50**
a. subclavia dextra	0.92 (0.18)	0.98 (0.22)	**5.24**
a. axillaris sinistra	0.88 (0.29)	0.92 (0.12)	**16.00**
a. axillaris dextra	0.79 (0.30)	0.94 (0.15)	**0.87**
a. vertebralis sinistra	0.90 (0.17)	0.85 (0.15)	**8.54**
a. vertebralis dextra	0.86 (0.18)	0.87 (0.23)	**24.00**
Ascending aorta	1.10 (0.08)	1.06 (0.06)	**8.35**
Aortic arch	1.07 (0.08)	1.06 (0.11)	**17.09**
Pulmonary arteries	1.09 (0.11)	1.08 (0.08)	**6.76**
Descending aorta	1.06 (0.07)	1.07 (0.09)	**23.12**
Abdominal aorta	1.10 (0.19)	1.09 (0.12)	**16.00**
Glandula parotis sinistra	1.34 (0.75)	1.02 (0.41)	**5.52**
Glandula parotis dextra	1.37 (0.78)	1.01 (0.43)	**3.35**
a. iliaca externa sinistra	1.03 (0.24)	1.04 (0.19)	**13.41**
a. iliaca externa dextra	0.95 (0.22)	1.05 (0.16)	**3.35**
a. femoralis sinistra	1.04 (0.25)	0.93 (0.19)	**9.75**
a. femoralis dextra	1.00 (0.20)	0.98 (0.26)	**18.20**
a. tibialis sinistra	1.02 (0.29)	0.93 (0.15)	**13.50**
a. tibialis dextra	0.99 (0.29)	0.96 (0.18)	**11.69**
Liver	1.47 (0.12)	1.34 (0.11)	**0.18**
m. brachioradialis sinistra	0.49 (0.14)	0.48 (0.23)	**14.59**
m. brachioradialis dextra	0.49 (0.16)	0.47 (0.11)	**18.20**

TBR = target to background ratio.

TVS [^{18}F]FDG-PET/CT analysis

Moderate agreement was obtained between the two observers (ICC = 0.65, $p < 0.001$), meaning we performed separate analyses for the two observers (figure 2). We found a mean TVS of 3.00 ± 2.42 (observer 1) and 4.46 ± 2.07 (observer 2) in the long COVID group versus 3.60 ± 2.45 (observer 1) and 5.12 ± 2.62 (observer 2) in the control group in the analysis of ten targets (long COVID group n = 13, control group n = 25), as is shown in table 3. No observer

reported a significant difference between the two groups (p=0.53 and p=0.52, respectively). We found a mean TVS of 8 ± 4.42 (observer 1) and 7.08 ± 3.66 (observer 2) in the long COVID group versus 9.56 ± 2.24 (observer 1) and 6.78 ± 3.35 (observer 2) in the control group in the analysis of thirteen targets (long COVID group n = 13, control group n = 9), as is shown in table 4. This yielded no significant differences for both observers (p = 0.37 and p = 0.92).

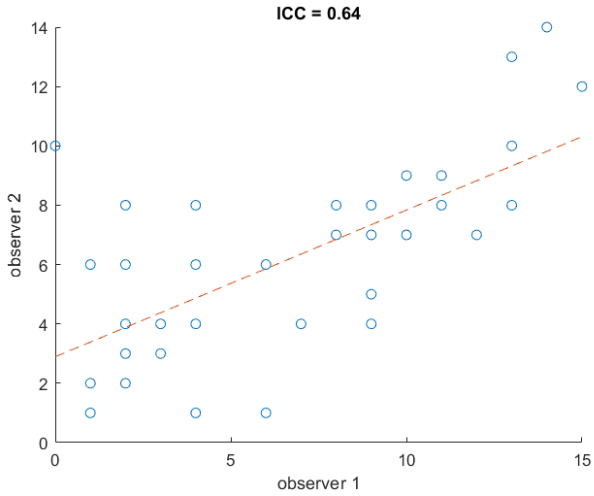

Figure 2. Scatterplot of TVS between the two observers. TVS = total vascular score, ICC = intraclass correlation coefficient.

Table 3. Total Vascular Score (TVS) in the long COVID group (n = 13) and control group (n = 26), 10 targets.

	TVS mean (std)	
	Observer 1	**Observer 2**
TVS long COVID group	3 (2.42)	4.46 (2.07)
TVS control group	3.60 (2.45)	5.12 (2.62)
p-value	0.53	0.52

Table 4. Total Vascular Score (TVS) in the long COVID group (n = 13) and control group (n = 9), 13 targets.

	TVS mean (std)	
	Observer 1	**Observer 2**
TVS long COVID	8.00 (4.42)	7.08 (3.66)
TVS control group	9.56 (2.24)	6.78 (3.35)
p-value	0.37	0.47

DISCUSSION

In this proof of concept study, we investigated the potential added value of [^{18}F]FDG-PET/CT for long COVID patients with persistent symptoms. No significant differences were found between the long COVID group and the control group in the semi-qualitative analysis and TVS. However, although several long COVID patients showed higher uptake in one or more of these targets, we were unable to identify a general pattern.

In a similar study performed by Sollini *et al*., a significant difference was found between the long COVID group and the control group in several targets, including the right femoral artery, the ascending aorta, aortic arch and the descending aorta [16]. However, no correction for multiple testing was performed and if applied, no significant differences would have been found. In the current study, the Bonferroni correction for multiple testing was used to prevent false positive findings [25]. If no Bonferroni correction had been applied, we would have found significant differences in the liver and the right axillary arteries between the long COVID group and control group (Supplementary table A), which illustrates the similarity of results between Sollini et al. and the current study.

However, it should be noted that long COVID presentation could be heterogeneous in nature, as other rheumatic diseases such as PMR also show high heterogeneity across patients on [^{18}F]FDG-PET/CT scans [26,27]. Furthermore, similar studies also found heterogeneous differences between long COVID patients and controls [28,29].

The liver has been reported as COVID-19 target organ [30,31] and recent studies suggest that the liver might be still inflamed in long COVID [29,32]. This possibly explains the higher liver uptake in the long COVID group compared to the control group.

The results of this study should be considered alongside certain limitations. Firstly, the study population consisted of 13 long COVID patients, limiting the power of the study. The control group could not be matched for age and sex to the long COVID group due to limitations in our database. Due to the large heterogeneity of [^{18}F]FDG-uptake within both groups, the TBR distributions overlapped between the two groups. This was an important cause for the high p-values we found in the semi-qualitative and TVS analyses.

Another limitation is that the image reconstruction was not EARL compliant since EARL specifications were not yet applied at the time of acquisition, which might have resulted in increased SUV variability [33]. Moreover, the time interval between [^{18}F]FDG injection and image acquisition was lower than 60 minutes in both groups due to logistic reasons, which deviates from the EANM recommendation for LVV and PMR, which Sollini *et al.* did

adhere to [16,22]. This may have had an impact on the results, although no guidelines on the recommended time interval between [18F]FDG injection and image acquisition have been published for long COVID patients and there were no significant differences in interval time between the two groups.

Moreover, the scanning window (whole-body imaging versus torso imaging) should be consistent for all subjects in order to be able to assess all locations [34]. Future studies should also consider specifying and quantifying the location of pain per patient.

It should also be noted that all measurements were manually performed and thus prone to errors [33]. Nonetheless, the nuclear medicine physicians (SB and RA) had a minimum of 5 years of experience and measurements were performed carefully, minimizing the number of random errors.

Little is known about long COVID and patients' management is still inconsistent due to lack of clinical practice guidelines. Furthermore, [18F]FDG-PET/CT data in long COVID patients was limited. Although our retrospective proof of concept study concerns only a small study population, we believe that our findings exhibit the complexity of the disease and add to the knowledge of the application of [18F]FDG-PET/CT in long COVID.

In summary, we found no quantitative difference in the TBR or TVS between long COVID patients and controls. Based on our results, we are unable to prove that [18F]FDG-PET/CT scans are of added value for long COVID patients with symptoms of myalgia or joint pain, reminiscent of vasculitis and PMR. To gain more insight in the underlying mechanisms of long COVID, prospective cohort studies are necessary.

REFERENCES

1. Shi Y, Wang G, Cai X, Deng J, Zheng L, Zhu H, et al. An overview of COVID-19. 2020;21(5):343–60.
2. Wang D, Hu B, Hu C, Zhu F, Liu X, Zhang J, et al. Clinical Characteristics of 138 Hospitalized Patients with 2019 Novel Coronavirus-Infected Pneumonia in Wuhan, China. JAMA - J Am Med Assoc. 2020;323(11):1061–9.
3. Yue H, Bai X, Wang J, Yu Q, Liu W, Pu J, et al. Clinical characteristics of coronavirus disease 2019 in Gansu province, China. Ann Cardiothorac Surg. 2020;9(4):1404–12.
4. Iqbal A, Iqbal K, Arshad Ali S, Azim D, Farid E, Baig MD, et al. The COVID-19 Sequelae: A Cross-Sectional Evaluation of Post-recovery Symptoms and the Need for Rehabilitation of COVID-19 Survivors. Cureus. 2021;2(2).
5. Wu Z, McGoogan JM. Characteristics of and Important Lessons from the Coronavirus Disease 2019 (COVID-19) Outbreak in China: Summary of a Report of 72314 Cases from the Chinese Center for Disease Control and Prevention. JAMA - J Am Med Assoc. 2020;323(13):1239–42.
6. Raveendran A V, Jayadevan R, Sashidharan S. Since January 2020 Elsevier has created a COVID-19 resource centre with free information in English and Mandarin on the novel coronavirus COVID- 19 . The COVID-19 resource centre is hosted on Elsevier Connect , the company ' s public news and information . 2020;(January).
7. Taquet M, Dercon Q, Luciano S, Geddes JR, Husain M, Harrison PJ. Incidence, co-occurrence, and evolution of long-COVID features: A 6-month retrospective cohort study of 273,618 survivors of COVID-19. PLoS Med [Internet]. 2021;18(9):1–22. Available from: http://dx.doi.org/10.1371/journal.pmed.1003773
8. Davis HE, Assaf GS, McCorkell L, Wei H, Low RJ, Re'em Y, et al. Characterizing long COVID in an international cohort: 7 months of symptoms and their impact. eClinicalMedicine. 2021;38.
9. Shaw B, Daskareh M, Gholamrezanezhad A. The lingering manifestations of COVID-19 during and after convalescence: update on long-term pulmonary consequences of coronavirus disease 2019 (COVID-19). Radiol Medica [Internet]. 2021;126(1):40–6. Available from: https://doi.org/10.1007/s11547-020-01295-8
10. Carfì A, Bernabei R, Landi F. Persistent Symptoms in Patients After Acute COVID-19. N Engl J Med. 2020;324(6):603–5.
11. Siddiqi HK, Libby P, Ridker PM. Since January 2020 Elsevier has created a COVID-19 resource centre with free information in English and Mandarin on the novel coronavirus COVID- 19 . The COVID-19 resource centre is hosted on Elsevier Connect , the company ' s public news and information. Trends. 2020;31(January):1–5.
12. Zacharias H, Dubey S, Koduri G, Cruz DD. Since January 2020 Elsevier has created a COVID-19 resource centre with free information in English and Mandarin on the novel coronavirus COVID-19 . The COVID-19 resource centre is hosted on Elsevier Connect , the company ' s public news and information . 2020;(January).
13. Derksen VFAM, Kissel T, Lamers-Karnebeek FBG, Van Der Bijl AE, Venhuizen AC, Huizinga TWJ, et al. Onset of rheumatoid arthritis after COVID-19: Coincidence or connected? Ann Rheum Dis. 2021;80(8):1096–8.
14. Viner R, Whittaker E. Kawasaki-like disease: emerging complication during the COVID-19 pandemic. 2020;(January).
15. Jamar F, Buscombe J, Chiti A, Christian PE, Delbeke D, Donohoe KJ, et al. EANM/SNMMI guideline for 18F-FDG use in inflammation and infection. J Nucl Med. 2013;54(4):647–58.

16. Sollini M, Ciccarelli M, Cecconi M, Aghemo A, Morelli P, Gelardi F, et al. Vasculitis changes in COVID-19 survivors with persistent symptoms: an [(18)F]FDG-PET/CT study. Eur J Nucl Med Mol Imaging. 2020/10/31. 2021;48(5):1460–6.

17. Sollini M, Morbelli S, Ciccarelli M, Cecconi M, Aghemo A, Morelli P, et al. Long COVID hallmarks on [18F]FDG-PET/CT: a case-control study. Eur J Nucl Med Mol Imaging. 2021/03/08. 2021;48(10):3187–97.

18. Rodríguez-Alfonso B, Ruiz Solís S, Silva-Hernández L, Pintos Pascual I, Aguado Ibáñez S, Salas Antón C. (18)F-FDG-PET/CT in SARS-CoV-2 infection and its sequelae. Rev Esp Med Nucl Imagen Mol (Engl Ed). 2021/08/04. 2021;40(5):299–309.

19. Pan T, Einstein SA, Kappadath SC, Grogg KS, Lois Gomez C, Alessio AM, et al. Performance evaluation of the 5-Ring GE Discovery MI PET/CT system using the national electrical manufacturers association NU 2-2012 Standard. Med Phys. 2019;46(7):3025–33.

20. Keyes Jr J. SUV: standard uptake or silly useless value? J Nucl Med [Internet]. 1995;36(10):1836–9. Available from: http://www.osti.gov/scitech/biblio/478317

21. Kinahan PE, Fletcher JW. Positron emission tomography-computed tomography standardized uptake values in clinical practice and assessing response to therapy. Semin Ultrasound, CT MRI. 2010;31(6):496–505.

22. Slart RHJA, Slart RHJA, Glaudemans AWJM, Chareonthaitawee P, Treglia G, Besson FL, et al. FDG-PET/CT(A) imaging in large vessel vasculitis and polymyalgia rheumatica: joint procedural recommendation of the EANM, SNMMI, and the PET Interest Group (PIG), and endorsed by the ASNC. Eur J Nucl Med Mol Imaging. 2018;45(7):1250–69.

23. Boellaard R, Krak NC, Hoekstra OS, Lammertsma A a, Jaskowiak CJ, Bianco J a, et al. Effects of Noise, Image Resolution, and ROI Definition on the Accuracy of Standard Uptake Values: A Simulation Study. J Nucl Med [Internet]. 2002;45(3):670–8. Available from: http://www.ncbi.nlm.nih.gov/pubmed/15750154%5Cnhttp://www.ncbi.nlm.nih.gov/pubmed/15347719

24. Sedgwick P. Multiple significance tests: The Bonferroni correction. BMJ. 2012;344(7841):1–2.

25. Curtin F, Schulz P. Multiple correlations and Bonferroni's correction. Biol Psychiatry. 1998;44(8):775–7.

26. Rehak Z, Sprlakova-Pukova A, Kazda T, Fojtik Z, Vargova L, Nemec P. (18)F-FDG PET/CT in polymyalgia rheumatica-a pictorial review. Br J Radiol. 2017/05/17. 2017;90(1076):20170198.

27. Rehak Z, Vasina J, Nemec P, Fojtik Z, Koukalova R, Bortlicek Z, et al. Various forms of (18)F-FDG PET and PET/CT findings in patients with polymyalgia rheumatica. Biomed Pap Med Fac Univ Palacky Olomouc Czech Repub. 2015/05/27. 2015;159(4):629–36.

28. Rodríguez-Alfonso B, Ruiz Solís S, Silva-Hernández L, Pintos Pascual I, Aguado Ibáñez S, Salas Antón C. (18)F-FDG-PET/CT in SARS-CoV-2 infection and its sequelae. Rev Esp Med Nucl Imagen Mol. 2021/07/28. 2021;40(5):299–309.

29. Sollini M, Morbelli S, Ciccarelli M, Cecconi M, Aghemo A, Morelli P, et al. Long COVID hallmarks on [18F]FDG-PET/CT: a case-control study. Eur J Nucl Med Mol Imaging. 2021/03/08. 2021;48(10):3187–97.

30. Maiese A, Manetti AC, La Russa R, Di Paolo M, Turillazzi E, Frati P, et al. Autopsy findings in COVID-19-related deaths: a literature review. Forensic Sci Med Pathol. 2020/10/08. 2021;17(2):279–96.

31. Libby P, Lüscher T. COVID-19 is, in the end, an endothelial disease. Eur Hear J. 2020/09/04. 2020;41(32):3038–44.

32. Bai Y, Xu J, Chen L, Fu C, Kang Y, Zhang W, et al. Inflammatory response in lungs and extrapulmonary sites detected by [(18)F] fluorodeoxyglucose PET/CT in convalescing COVID-19 patients tested negative for coronavirus. Eur J Nucl Med Mol Imaging. 2021/01/10. 2021;48(8):2531–42.

33. Kaalep A, Burggraaff CN, Pieplenbosch S, Verwer EE, Sera T, Zijlstra J, et al. Quantitative implications of the updated EARL 2019 PET–CT performance standards. EJNMMI Phys. 2019;6(1):1–16.

34. Lensen KJDF, Van Sijl AM, Voskuyl AE, Van Der Laken CJ, Heymans MW, Comans EFI, et al. Variability in quantitative analysis of atherosclerotic plaque inflammation using 18F-FDG PET/CT. PLoS One. 2017;12(8):1–14.